Detection of Nitrogen and Neon in the X-ray Spectrum of GP Com with *XMM/Newton*

Tod E. Strohmayer

Laboratory for High Energy Astrophysics, NASA's Goddard Space Flight Center, Greenbelt, MD 20771; stroh@clarence.gsfc.nasa.gov

ABSTRACT

We report on X-ray spectroscopic observations with *XMM/Newton* of the ultracompact, double white dwarf binary, GP Com. With the Reflection Grating Spectrometers (RGS) we detect the Lα and Lβ lines of hydrogen-like nitrogen (N VII) and neon (Ne X), as well as the helium-like triplets (N VI and Ne IX) of these same elements. All the emission lines are unresolved. These are the first detections of X-ray emission lines from a double-degenerate, AM CVn system. We detect the resonance (r) and intercombination (i) lines of the N VI triplet, but not the forbidden (f) line. The implied line ratios for N VI, $R = f/i < 0.3$, and $G = (f + i)/r \approx 1$, combined with the strong resonance line are consistent with formation in a dense, collision-dominated plasma. Both the RGS and EPIC/MOS spectra are well fit by emission from an optically thin thermal plasma with an emission measure (EM) $\propto (kT/6.5 \text{ keV})^{0.8}$ (model *cevmkl* in XSPEC). Helium, nitrogen, oxygen and neon are required to adequately model the spectrum, however, the inclusion of sulphur and iron further improves the fit, suggesting these elements may also be present at low abundance. We confirm in the X-rays the underabundance of both carbon and oxygen relative to nitrogen, first deduced from optical spectroscopy by Marsh et al. The average X-ray luminosity of $\approx 3 \times 10^{30}$ ergs s^{-1} implies a mass accretion rate $\dot{m} \approx 9 \times 10^{-13}$ $M_\odot$ yr^{-1}. The implied temperature and density of the emitting plasma, combined with the presence of narrow emission lines and the low $\dot{m}$ value, are consistent with production of the X-ray emission in an optically thin boundary layer just above the surface of the white dwarf.

Subject headings: Binaries: general - Stars: individual (GP Com) - Stars: white dwarfs - cataclysmic variables - X-rays: stars - X-rays: binaries

1. Introduction

The AM CVn stars are among the most compact binary systems known. Their optical spectra are dominated by broad helium emission lines originating in an accretion disk formed by mass transfer from a degenerate helium dwarf onto the primary white dwarf. Their orbital periods range from about 10 minutes to 1 hour. They are natural laboratories for the study of poorly understood binary evolution processes, such as common envelope evolution. Moreover, the absence of hydrogen allows for the study of accretion disks dominated by helium. They may also be a significant channel for the production of Type Ia supernovae and neutron stars via accretion induced collapse (for a review see Warner 1995).

GP Com is one of the better studied, nearby AM CVn systems. It has a 46.5 minute orbital period (Nather Robinson & Stover 1981), resides at a distance of ≈ 70 pc (Thorstensen 2003), and has been studied extensively in the optical and UV. Recent studies by Marsh (1999) and Morales-Rueda et al.(2003) have used optical and UV+optical spectroscopy to probe the dynamics of the system in great detail. In addition to helium, nitrogen emission lines have been seen in the UV (Lambert & Slovak 1981; Marsh et al. 1995), and optical (Marsh, Horne & Rosen 1991). These observations identified a nitrogen overabundance, relative to carbon and oxygen, as well as an underabundance of heavy elements (for example, Ca, Si and Fe). The low metallicity may be consistent with its suggested halo origin (see Giclas, Burnham & Thomas 1961). The evolution scenario favored by Marsh et al. (1991) posits an initially low metallicity for the progenitor stars. The CNO elements are subsequently produced within the primary star and then mixed throughout the secondary during a common envelope phase. The nitrogen abundance is then increased by CNO-cycle hydrogen burning within the secondary (ie. the mass donor). Finally, a number of ultracompact systems with neutron star primaries also show apparent neon enrichment (see Juett & Chakrabarty 2003; Schulz et al. 2001).

Accretion should make such systems soft X-ray sources, and indeed, several have been detected in the X-ray band, including the prototype AM CVn, CR Boo, and GP Com (van Teeseling & Verbunt 1994; Ulla 1995; and Eracleous, Halpern & Patterson 1991). The X-ray flux from accreting, non-magnetic white dwarfs is thought to originate in a boundary layer that shocks and decelerates the Keplerian flow, allowing it to eventually settle on the white dwarf. Early work suggested that the boundary layer should be optically thick–radiating in the soft X-ray band and extreme UV–at mass accretion rates above $\dot{m} \approx 1.6 \times 10^{-10} M_{\odot}$ yr^{-1} (Pringle & Savonije 1979). At lower rates the boundary layer should become more radially extended and optically thin, producing a harder X-ray spectrum. Aspects of this basic scenario have been confirmed by more recent calculations (see, for example, Patterson & Raymond 1985; Narayan & Popham 1993; Popham & Narayan 1995).

To date, X-ray observations of most AM CVn systems have been made at relatively low signal to noise levels and with modest spectral resolution. For example, ROSAT observations of GP Com found the source at a flux level $\approx 1.2 \times 10^{-11}$ ergs cm^{-2} s^{-1} in the 0.2 - 2 keV band, and confirmed that it is variable. These observations also found that the 0.2 - 2 keV spectrum cannot be described by a single temperature component (van Teeseling & Verbunt 1994), but detailed modelling was problematic due to the relatively poor statistics and restricted bandpass.

In this Letter we summarize results of recent, high signal to noise X-ray spectral measurements of GP Com with *XMM/Newton*. These data represent perhaps the best X-ray spectral measurements of an AM CVn system to date, and also show the first X-ray emission lines from such a system.

2. XMM Observations

XMM/Newton observed GP Com for 56.5 ksec beginning on January 3, 2001. The EPIC observations were done in imaging mode. We used version 5.4.1 of the XMM software (SAS) to analyze the data. GP Com was easily detected at the few counts s^{-1} level in the EPIC instruments. A lightcurve combining data from the PN and MOS detectors is shown in Figure 1, and confirms substantial X-ray variability, including several 2 to 4 minute flares during which the X-ray flux increased by factors of 2 - 3. Flaring has often been seen in the UV and optical, particularly in the N V (1240$\mathring{A}$) resonance line (Marsh et al. 1995). We will present a detailed timing study of GP Com in a subsequent paper. We extracted spectra and produced response files for each of the instruments using the relevant SAS tools.

2.1. Spectral Analysis: RGS and EPIC/MOS

The spectrum extracted from both RGS instruments is shown in Figure 2, along with identifications for all the strongest line features. The strongest detected feature is the Lyα line of hydrogenic nitrogen (N VII) at 24.78 $\mathring{A}$, but other lines of nitrogen are also present, including the Lyβ line as well as the helium-like triplet of N VI at $\approx 29\mathring{A}$. The only other signifcant line features are due to neon. The hydrogenic Lyα and Lyβ lines as well as the helium-like triplet are detected. Particularly striking is the absence of any strong carbon or oxygen lines in the spectrum.

We fit the observed line features using Lorentzian profiles with the widths fixed at that of the RGS line spread function (LSF) for that wavelength (see den Herder et al. 2001; Pollock

et al. 2003). All the hydrogenic lines are well fit with such a profile and are unresolved. Table 1 summarizes the salient properties of all the detected lines.

As is well known, the helium-like triplets can be used as probes of the plasma where the lines are produced (see Gabriel & Jordan 1969; Porquet & Dubau 2000). The line flux ratios, $R = f/i$, and $G = (i + f)/r$, of the resonance (r), intercombination (i) and forbidden (f) transitions are sensitive to the electron density and temperature of the plasma, respectively. For each triplet we fit a Lorentzian profile at the rest wavelength of each transition. To determine the line ratios, we fixed the wavelength and width of each line, but allowed the line fluxes to vary. The signal to noise ratio in both triplets is not particularly high, but the line ratios can at least be roughly estimated. The nitrogen triplet is better resolved than that of neon. The results of our fits are shown in Figure 3 (see also Table 1). For the N VI triplet we detect the resonance and intercombination lines, but interestingly, not the forbidden line. The line ratios for N VI, $R = f/i < 0.3$, and $G = (f + i)/r \approx 1$, and the strong resonance line are consistent with formation in a dense, collision-dominated plasma (Porquet & Dubau 2000). For nitrogen, a strong UV radiation field can also decrease the strength of the forbidden line, mimicking a density effect, however, the line ratios from the neon triplet–which are much less sensitive to radiation field effects–are also consistent with a plasma at or near the critical density $n_c = 5.3 \times 10^9$ cm^{-3} for nitrogen.

We fit the EPIC/MOS and RGS spectra with several collisional ionization equilibrium (CIE) plasma emission models. We found that multi-temperature models fit the data significantly better than single temperature models. For example, the multi-temperature and variable abundance model *cevmkl* in XSPEC (version 11.3) provides an excellent fit to the data from both the RGS and EPIC instruments (see Mewe, Gronenschild & van den Oord 1985; Mewe, Lemen & van den Oord 1986; Liedahl, Osterheld & Goldstein 1995). This model uses a power law in temperature for the emission measure distribution (EM), vis., EM $\propto (kT/kT_{max})^{\gamma}$, where kT_{max} and γ are the maximum temperature and power law index, respectively.

There is some evidence for modest pile-up in the PN spectra, so for the broad-band modeling we focused on the MOS data only. Figure 4 shows our best fit to the EPIC/MOS data using the *cevmkl* model. The model fits the data well, with a minimum χ^2 of 1,005 for 1,045 degrees of freedom. Using the MOS data only, the best-fit emission measure distribution is characterized by $kT_{max} = 6.3 \pm 0.3$ keV, and $\gamma = 0.85 \pm 0.05$. The 0.3 - 10 keV fluxes are 4.7 and 5.3×10^{-12} ergs cm^{-2} s^{-1} in the MOS1 and MOS2, respectively. Taking the mean, we arrive at an average luminosity (at 70 pc) of 2.94×10^{30} ergs s^{-1} in the same band.

The elements strongly required by the fit are helium, nitrogen, oxygen and neon, how-

ever, χ^2 additionally improves by 13.35 and 23.9 with the inclusion of iron and sulphur, respectively, suggesting these elements may also be present at low abundance. No other elements are required to fit the spectrum. Using this model we determined the abundances relative to the solar values tabulated by Anders & Grevesse (1989). Expressed as mass fractions we find; $X_{He} = 0.977 \pm 0.002$, $X_N = 1.7 \pm 0.1 \times 10^{-2}$, $X_O = 2.2 \pm 0.3 \times 10^{-3}$, $X_{Ne} = 3.7 \pm 0.2 \times 10^{-3}$, $X_S = 2.3 \pm 0.6 \times 10^{-4}$, and $X_{Fe} = 8 \pm 2 \times 10^{-5}$. In addition, we placed limits (3σ) on several prominent elements which were not detected; $X_C < 2 \times 10^{-3}$, $X_{Mg} < 1.6 \times 10^{-4}$ and $X_{Si} < 8 \times 10^{-5}$. Our limits on some of the heavier metals (such as Si, Mg, and Fe) suggest underabundances compared with solar values. This is qualitatively similar to the abundances derived from optical spectroscopy (Marsh et al. 1991).

3. Discussion

The nitrogen lines in the X-ray band provide additional confirmation of the overabundance of nitrogen relative to carbon and oxygen deduced from the optical (Marsh et al. 1991). The high nitrogen abundance likely reflects the operation of CNO-cycle thermonuclear processing in the secondary (Marsh et al. 1991). We find a nitrogen to helium ratio, by number, of $\approx 4.8 \times 10^{-3}$, which is moderately higher than the value derived by Marsh et al. (1991) of 2.7×10^{-3} (see their Table 4). Our derived oxygen to helium number ratio is, however, about a factor of 10 higher than that deduced from the optical. Although systematic modelling effects could be present, these results suggest that the X-ray emitting gas may have higher oxygen abundance than the accretion disk (which produces the optical emission lines). If the accretor were an oxygen-rich white dwarf, and some of its matter is mixed with the accreted material in the turbulent boundary layer, then this could perhaps increase the oxygen abundance relative to the donor material.

The neon lines provide the first definitive detection of an element heavier than oxygen in GP Com. Our derived neon mass fraction (≈ 0.0037) is a factor of 2 larger than the solar value. Moreover, modelling of the optical spectra also suggests a neon enrichment of about 1.3 compared to solar abundances (Marsh et al. 1991). Neon is a by-product of helium burning under a wide range of conditions (see, for example, Clayton 1983; Iben & Truran 1983), however, the low carbon abundance is likely incompatible with helium burning having ocurred in the secondary. Therefore, this avenue for the neon production appears to be a dead-end. Again, mixing of neon from the accretor (which likely has undergone helium burning) into the donor material in the boundary layer could perhaps increase the neon abundance. It appears that gravitational settling and fractionation of neon (in the form of ^{22}Ne) are also not relevant, since nitrogen is depleted in the production of this isotope, and

we clearly measure a large nitrogen abundance (see, for example, Bildsten & Hall 2001).

Neon enhancements have been suggested for several ultracompact neutron star binaries; 4U 1543-624 and 2S 0918-549 (Juett & Chakrabarty 2003), and 4U 1627-67 (Schulz et al. 2001). For 4U 1543-624, Juett & Chakrabarty (2003) deduced Ne/O ≈ 1.5, by number, from studies of absorption edges in *Chandra* high resolution spectra, however, we note that these measurements can be influenced by the unknown ionization structure in the circumbinary material. We find a similar value of Ne/O = 1.4 (by number) for GP Com. Yungelson, Nelemans & van den Heuvel (2002) suggest fractionation of neon in the white dwarf donor as a possible explanation for the neon enhancements in the neutron star systems. This scenario again requires a helium burning donor and thus seems not to work in the case of GP Com.

The X-ray measurements provide a means to estimate the mass accretion rate, $\dot{m}$, onto the white dwarf primary in GP Com. Assuming matter falls from the inner Lagrange point onto the primary, and that half the gravitational potential energy is dissipated in the accretion disk, the X-ray luminosity, L_x can be approximated as (see, for example, Nelemans, Yungelson & Portegies Zwart 2004),

$$L_x = \frac{1}{2}\frac{GM_1\dot{m}}{R}\left(1 - \frac{R}{R_{L_1}}\right) , \tag{1}$$

where M_1, R, R_{L_1}, and $\dot{m}$ are the primary mass, primary radius, the distance from the inner Lagrange point to the center of the accretor, and the mass accretion rate, respectively. Solving for $\dot{m}$, and inserting the measured X-ray luminosity for L_x gives,

$$\dot{m} = 3.48 \times 10^{-13}\frac{R_9}{(M_1/M_\odot)}\left(1 - \frac{R}{R_{L_1}}\right)^{-1} \; M_\odot \; \mathrm{yr}^{-1} , \tag{2}$$

where R_9 is the radius of the primary in units of 10^9 cm, and $R/R_{L_1} \approx 0.2$ for a system like GP Com. For a primary mass, $M_1 = 0.5M_\odot$ (Morales-Rueda et al. 2003) and $R_9 = 1$ (Zapolsky & Salpeter (1969) we obtain $\dot{m} \approx 8.7 \times 10^{-13}$ $M_\odot$ yr^{-1}. If the accretor is a massive O/Ne/Mg white dwarf (suggested by the possibility of oxygen and neon mixing in the boundary layer), then the derived accretion rate drops by about a factor of 6.

This rate is substantially lower than the critical rate above which one expects an optically thick boundary layer (Pringle & Savonije 1979; Narayan & Popham 1993). In this regime the plasma should have a maximum temperature of $\approx 10^8$ K, which is similar to the peak temperature of 6.5 keV (7.5×10^7 K) deduced from our spectral modelling. The presence of *narrow* emission lines also supports spectral formation in a boundary layer. From the width of the N VII Lyα line, we obtain an upper limit on the velocity dispersion of the emitting gas of ≈ 250 km s^{-1} (3σ) (This includes bulk and thermal motions). This indicates an origin

close to the white dwarf and not, for example, further out in the accretion disk, which would have much higher Keplerian velocities. If the white dwarf accretor was synchronized with the orbit, then its rotational velocity would be ≈ 23 km s^{-1}. To have a rotational speed equal to our 250 km s^{-1} limit, a 10^4 km white dwarf would require a spin period of ≈ 250 seconds. Indeed, an upper limit to the Doppler (ie. thermal motion) width for the nitrogen line indicates a value close to t250 km s^{-1}, which supports a slowly rotating, or synchronized white dwarf. The narrowness of the X-ray lines also appears consistent with the narrow "central spike" component of the helium lines (Marsh 1999; Morales-Rueda et al. 2003), which almost certainly originate on the accreting white dwarf.

The XMM/Newton measurements provide a detailed look at the physics of the boundary layer in GP Com. Detailed comparisons with theoretical boundary layer models could provide interesting constraints on their temperature, density and rotational profiles. Deeper X-ray spectra would provide better temperature and density constraints from the helium-like triplets, and likely more lines of less abundant species could be detected.

The author thanks Richard Mushotzky, Martin Still, Craig Markwardt, and the referee, Tom Marsh, for many useful comments and suggestions.

References

Anders E. & Grevesse N. 1989, Geochimica et Cosmochimica Acta 53, 197.

Bildsten, L. & Hall, D. M. 2001, ApJ, 549, L219.

Clayton, D. D. 1983, "Principles of Stellar Evolution and Nucleosynthesis," (Univ. of Chicago Press: Chicago).

Eracleous, M., Halpern, J. & Patterson, J. 1991, ApJ, 382, 290.

den Herder, J. W. et al. 2001, A&A, 365, L7.

Gabriel, A. H. & Jordan, C. 1969, MNRAS, 145, 241.

Giclas, H. L., Burnham, R., Jr., & Thomas, N. G. 1961, Lowell Obs. Bull., 112, 61.

Iben, I. & Truran, J. W. 1978, ApJ, 220, 980.

Juett, A. M. & Chakrabarty, D. 2003, ApJ, 599, 498.

Lambert, D. L. & Slovak, M, H. 1981, PASP, 93, 477.

Liedahl, D.A., Osterheld, A.L., and Goldstein, W.H. 1995, ApJL, 438, 115

Marsh, T. R., Wood, J. H., Horne, K. & Lambert, D. 1995, MNRAS, 274, 452.

Marsh, T. R., Horne, K. & Rosen, S. 1991, ApJ, 366, 535.

Marsh, T. R. 1999, MNRAS, 304, 443.

Mewe, R., Gronenschild, E.H.B.M., & van den Oord, G.H.J. 1985, A&AS, 62, 197.

Mewe, R., Lemen, J.R., & van den Oord, G.H.J. 1986, A&AS, 65, 511.

Morales-Rueda, L. et al. 2003, A&A, 405 249,

Narayan, R. & Popham, R, G. 1993, Nature, 362, 820.

Nather, R. E., Robinson, E. L. & Stover, R. J. 1981, ApJ, 244, 269.

Nelemans, G., Yungelson, L. R., & Portegies Zwart, S. F. 2004, MNRAS, 349, 181.

Patterson, J. & Raymond, J. C. 1985, ApJ, 292, 535.

Pollock, A. M. T. et al. 2003, XMM Calibration Document, XMM-SOC-CAL-TN-0030 Issue 2, "Status of the RGS Calibration,"

Popham, R. G. & Narayan, R. 1995, ApJ, 442, 337.

Porquet, D. & Dubau, J. 2000, A&AS, 143, 495.

Pringle, J. E. & Savonije, G. J. 1979, MNRAS, 187, 777.

Schulz, N. S. et al. 2001, ApJ, 563, 941.

Thorstensen, J. R. 2003, AJ, 126, 3017.

Ulla, A. 1995, A&A, 301, 469.

van Teeseling, A. & Verbunt, F. 1994, A&A, 292, 519.

Warner, B. 1995, *Cataclysmic Variable Stars*, Cambridge Univ. Press, Cambridge UK.

Yungelson, L. R., Nelemans, G. & van den Heuvel, E. P. J. 2002, A&A, 388, 546.

Zapolsky, H. S. & Salpeter, E. E. 1969, ApJ, 158, 809.

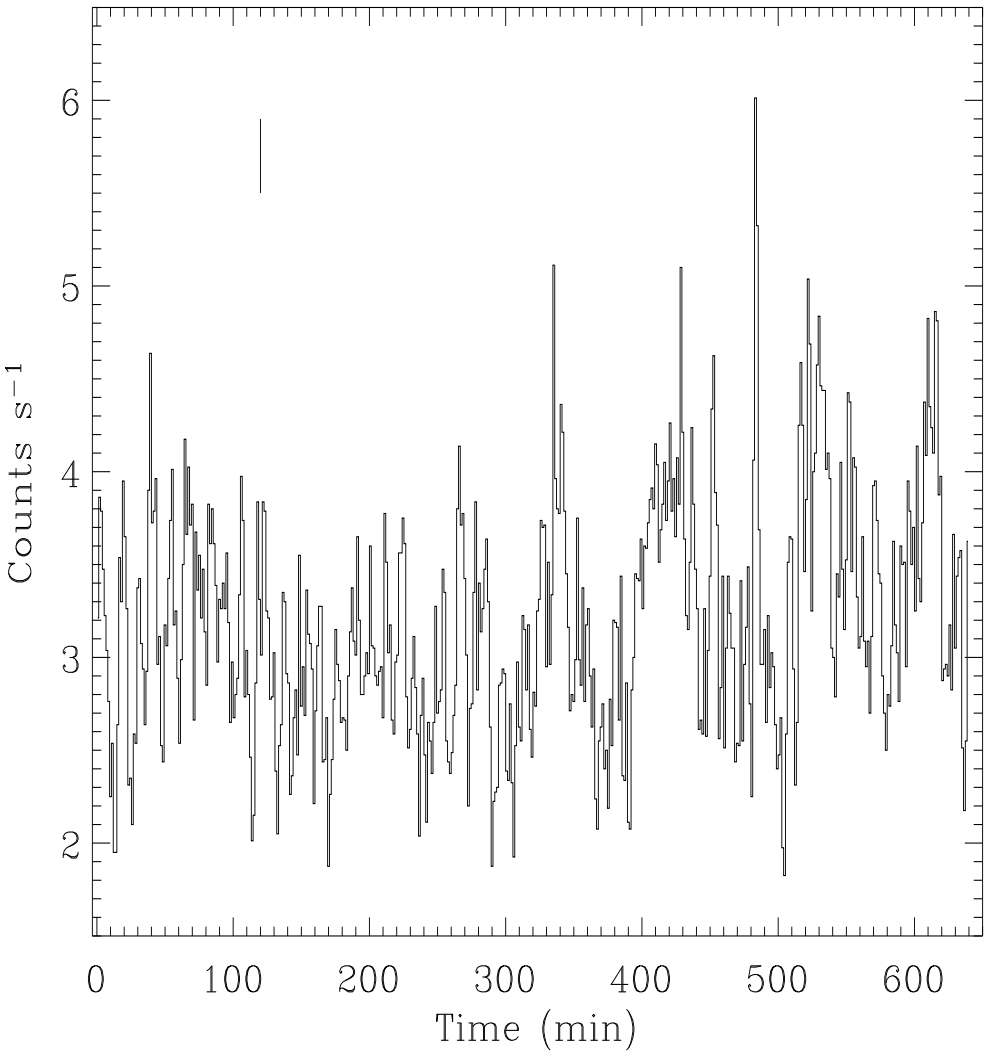

Figure 1: A lightcurve of a portion of the *XMM/Newton* EPIC (PN+MOS) observation of GP Com. The binsize is 80 s. Significant variability is evident on a range of timescales. A characteristic error bar is also shown (upper left).

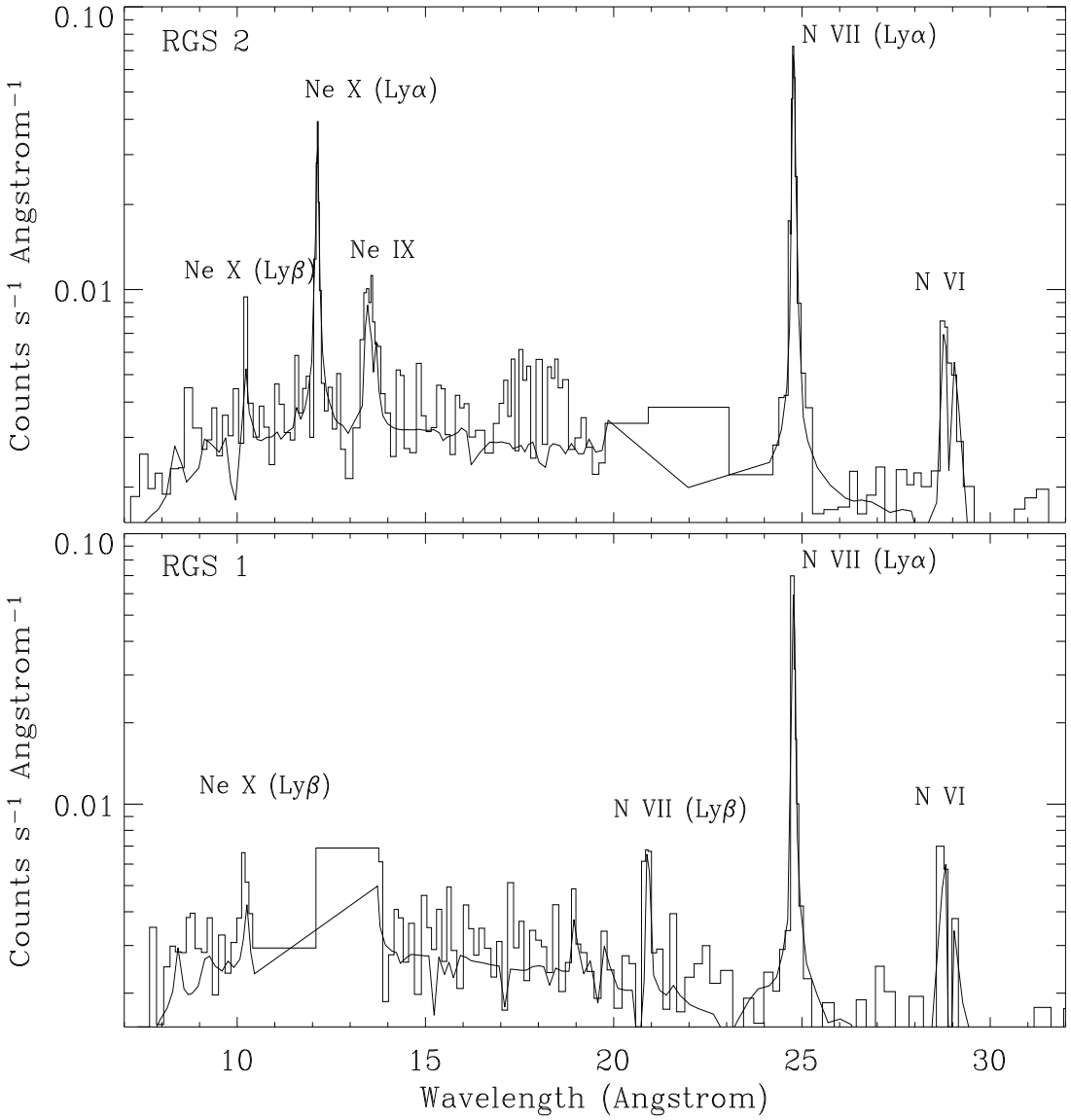

Figure 2: High resolution spectra of GP Com obtained with the RGS1 (bottom) and RGS2 (top) spectrometers in the $7 - 32$ $\mathring{A}$ band (solid histogram). Identifications are given for the prominent lines. The best fitting, variable emission measure plasma model (cevmkl in XSPEC) is also shown (solid curve).

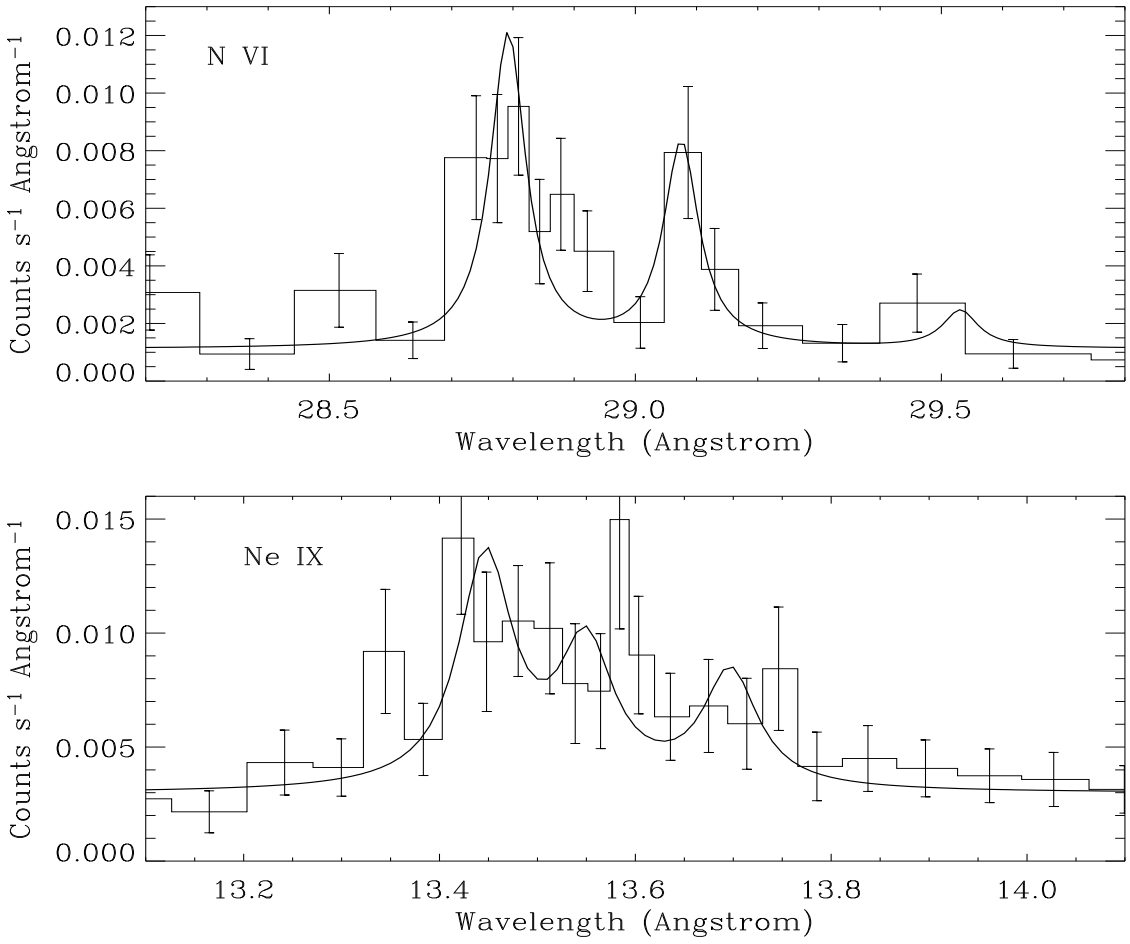

Figure 3: RGS spectra and best fitting Lorentzian line profiles for the N VI (top) and Ne IX (bottom) helium-like triplets.

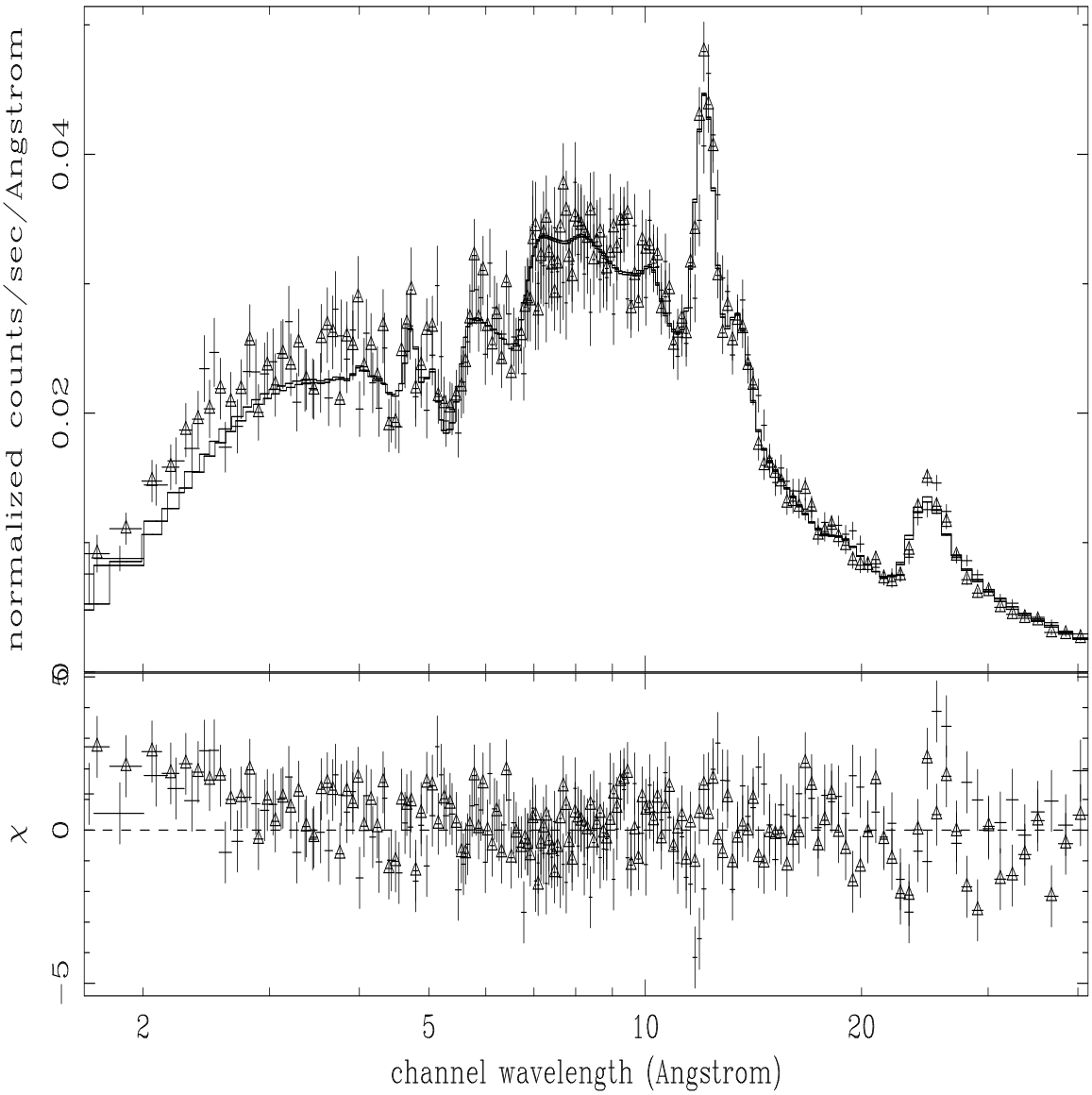

Figure 4: Phase-averaged spectrum of GP Com as observed in the EPIC/MOS detectors (MOS1:triangles, MOS2:crosses). Shown are the data and best fitting *cevmkl* model versus wavelength using XSPEC. The fit includes contributions from helium, nitrogen, oxygen, neon, sulphur and iron.

Table 1: Emission Line Properties for GP Com

Species	λ ($\AA$)			Flux	
	r	i	f	(10^{-4} cm^{-2} s^{-1})	
N VII		24.781		1.86	
N VII		20.910		0.28	
N VI	28.792	29.075	29.531	0.34	0.22	0.07[1]
Ne X		12.134		0.54	
Ne X		10.239		0.16	
Ne IX	13.447	13.550	13.697	0.20	0.11	0.09

[1] Not detected. 1σ upper limit.